Research Article

Chemical Review and Letters
journal homepage: www.chemrevlett.com
ISSN (online): 2645-4947 (print) 2676-7279

Docking Simulations and Virtual Screening to find Novel Ligands for T3S in Yersinia pseudotuberculosis YPIII, A drug target for type III secretion (T3S) in the Gram-negative pathogen Yersinia pseudotuberculosis

Emmanuel Israel Edache[a, b, *], Adamu Uzairu[b], Paul Andrew Mamza[b], Gideon Adamu Shallangwa[b]

[a]*Department of Pure and Applied Chemistry, University of Maiduguri, Borno State, Nigeria*
[b]*Department of Chemistry, Ahmadu Bello University, Zaria, Nigeria*

ARTICLE INFO

Article history:
Received 29 October 2020
Received in revised form 3 February 2021
Accepted 11 February 2021
Available online 7 May 2021

Keywords:
Molecular docking
Molecular dynamics simulation
ADME
Chlamydia
Y. pseudotuberculosis

ABSTRACT

An aggregate use of molecular docking, molecular dynamics simulations, and ADMET was successfully used to create salicylidene acyl hydrazides as inhibitors of type III secretion (T3S) in the Gram-negative pathogen Yersinia pseudotuberculosis and Chlamydia. Molecular docking study was performed on the simulated protein of cytidine monophosphate (CMP) which helped to correlate interactions of amino acids encompassed to the ligand. Molecular dynamics simulations study uncovered that the A-chain of CMP protein was stable at and above 100ps concerning temperature, Total energy, and kinetic energy. Virtual screening was executed dependent on pharmacophore modeling and molecular docking to distinguish the new inhibitors. Ten top-ranked compounds were discovered based on the Rerank score fitness function. ADME studies were executed on compounds retrieved from virtual screening in compliance with the standard ranges. All the results can offer us more valuable evidence for our further drug design.

1. Introduction

Diseases brought about by microorganisms have expanded seriously during the previous years. The bacteria have remained the reason for probably the most deadly diseases and well-known epidemics of human development [1]. Bacterial infections, for example, tuberculosis, Chlamydia, Y. pseudotuberculosis, typhus, plague, diphtheria, typhoid fever, cholera, looseness of the bowels, and pneumonia have taken a compelling expense on mankind [2]. Yersinia pseudotuberculosis is one of three human pathogenic members from the species, the others being Yersinia enterocolitica and Yersinia pestis. While Y. pseudotuberculosis and Y. enterocolitica are enteric pathogens, Y. pestis causes bubonic and pneumonic plague [3]. Yersinia pestis is viewed as a recently developed clonal subsidiary of Y. pseudotuberculosis [4]. This is a lethal infection brought about by microorganisms of the class mycobacterium which influences people [5]. Chlamydia is an explicitly transmitted bacterial disease. Chlamydia is a sexual transmitted disease (STD) brought about by Chlamydia trachomatis (C. trachomatis) [1]. This bacterium only infects humans. It affects both men and women and is spread during sexual contact [6]. As indicated by the Centers for Disease Control and Prevention (CDC), in 2015, there were over 1.5 million instances of chlamydia in the United States [7]. A pace of 478.8 cases per 100,000 populace, which has been expanding since 2001 [7]. Chlamydia has been the most widely recognized explicitly transmitted disease (STI) answered by the CDC. The World Health Organization (WHO) conjectures that there are more than 1 million new STDs procured every day all around [1]. People between the ages of 15 and 24 years gain half of every new STD, and 1 out of 4 explicitly dynamic immature females have an STD [6]. Centers for Disease Control and Prevention (CDC), in 2015, basically 3 percent of young ladies aged 15 to 19 years had chlamydia [7]. However, STD rates among seniors are increasing. Mortality increase caused by infectious diseases is directly identified with the bacteria that have multiple resistance to antibiotics [8]. The advancement of new antibacterial medications improved by innovatory and more effective mechanisms of action is an earnest clinical need. The Y. pseudotuberculosis and hostile to chlamydia drugs are decades old and are by and large immediately exhausted due to resistance. While clear, we need new bactericidal

* Corresponding author. Tel.: +2348066776802; e-mail: edacheson2004@gmail.com

antibiotics with novel mechanisms of action that kill replicating and non-replicating bacteria resulting in overall treatment shortening, it is basic that future medication advancement address some different elements. Some previous reports about the agreements between theoretical and computational results may be useful for increasing the trustability of the research [9-11]. Recent researches have discussed docking and molecular dynamics methods based on anti-bacterial [12, 13]. Also, some review papers that revealed about the usefulness of docking simulations in controlling the pandemics (like COVID-19) [14, 15]. We used a combination of molecular docking, molecular dynamic simulation, Effective selection of compounds with favorable absorption, distribution, metabolism, elimination and toxicology (ADMET) [16], are helpful computational methods for drug design [17, 18]. In molecular docking and molecular dynamic simulation, the 3D structure of the receptor will be accessible and receptor-ligand interactions play an important role, so this drug design is called structure-based drug design [19]. Docking is a method that proposes the favored orientation and energy of one ligand when bound in the active site to build a stable complex [20]. The molecular docking methodology was applied to a series of 58 salicylidene acylhydrazides derivatives, as inhibitors of type III secretion (T3S) in the Gram-negative pathogen Yersinia pseudotuberculosis and Chlamydia trachomatis to mimic the binding of analogs at the active site. Investigation of the basic attributes and interactions of the ligands was done to assess how the inhibitory movement is influenced by its properties. Molecular dynamics (MD) simulation are among the most frequently used SBDD strategies because of their wide extent of uses in the investigation of molecular recognition procedures such as binding energetics, molecular interactions, and induced conformational changes [21]. The multi-parameter optimization (MPO) strategies used to gauge drug-likeness and discover compounds with a decent parity of the many physicochemical and biological properties necessary to become an effective, useful, and nontoxic drug [22]. In the MPO techniques, we completed dependable guidelines including Lipinski and Veber rules [23, 24], and calculated metrics. On the other side, the calculated metrics method is the calculation of lipophilicity indices. The MPO desirability scores enhance the odds of identifying compounds with drug-like ADME and safety while maintaining good blood-brain barrier (BBB) penetration [25]. The Golden Triangle [26] is a visual image tool to simultaneously optimize drug absorption and clearance. By plotting the molecular weight concerning the distribution coefficient at pH 7.4 (log D 7.4) in this case MlogP and S+logD were used for a series of molecules. In our present research, we determined the MPO desirability score and golden triangle rule, we finished with the calculation of drug-likeness properties of a bioactive series of salicylidene acylhydrazides derivatives. The focus of these calculations is to identify compounds with drug-like ADME and safety attributes, great ability to penetrate the blood-brain barrier (BBB), for designing a successful Yersinia pseudotuberculosis and Chlamydia trachomatis drug.

2. Results and Discussion

Docking simulations is an optimization problem, where the goal is accomplished by producing a few adaptations (or poses) of ligands within the active site of the receptor and scoring them to recognize the best binding conformation [34, 35]. MVD unexpectedly distinguishes conceivable restricting locales (also referred to as cavities or active sites) by utilizing its cavity detection algorithm. The cavities within a 16.02 x -10.92 x 1.73Å3 centered at the experimentally known ligand position were utilized. The cavities that are identified by the cavity detection algorithm are then used by the guided differential evolution search algorithm to center the pursuit, to that particular region during the docking simulation. It was able to determine toward active site (Fig. 1), in cavity 1 (volumes: 484.864) and surface = 1335.04 and use protein A (pdb code: 4e22) of cytidine monophosphate (CMP) kinase structure crystalline. The techniques can be said legitimate if RMSD presented the least value [36]. The value of MolDock Score, Rerank Score, H-bond Score, and pIC50 parameters are presented in Table 1.

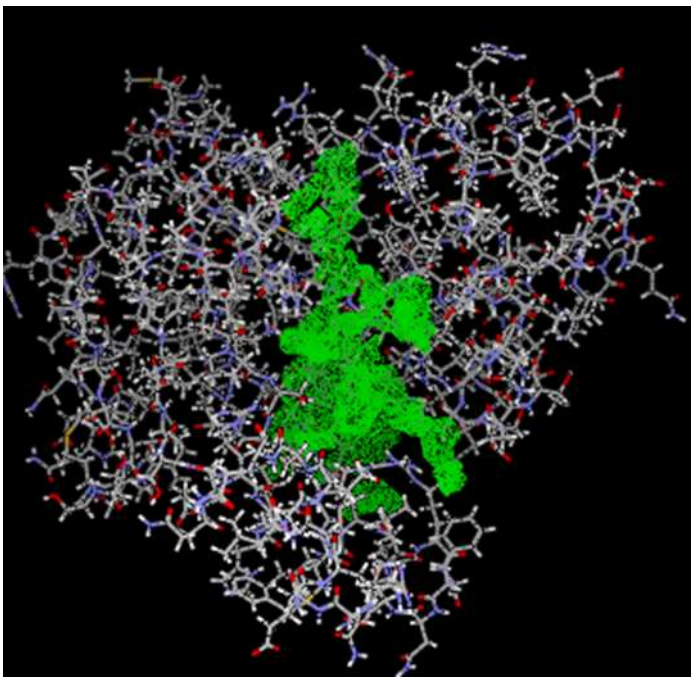

Figure 1: Crystal structure of cytidine monophosphate (CMP) kinase complex that binds to the ligand in the cavity (green) (PDB: 4e22).

Table 1. PubChem number, MVD results and corresponding activity pIC_{50} of salicylidene acylhydrazides derivatives.

compound	PUBCHEM_CID	MolDock Score	Rerank Score	HBond	pIC50
1	135804387	-103.976	-82.7862	-7.84729	8.00000
2	135504477	-103.005	-85.6211	-7.4875	7.823909
3	135480441	-96.9194	-78.4654	-7.40755	7.366532
4	136167947	-108.505	-89.1572	-8.32087	7.69897
5	136167948	-105.388	-93.2704	-9.68735	7.721246
6	136167949	-96.585	-83.1144	-8.80528	7.468521
7	136167950	-90.0098	-78.7496	-6.35355	7.568636
8	136167951	-82.2417	-75.9823	-6.9813	7.69897
9	136167952	-100.14	-77.3499	-10.6039	7.508638
10	136167953	-108.855	-86.3738	-5.92233	7.537602
11	136167954	-93.6028	-76.7005	-5.87577	7.60206
12	136167955	-114.008	-92.451	-5.60081	7.522879
13	136167956	-115.823	-96.1018	-4.47525	7.677781
14	136167957	-106.137	-87.4367	-3.72515	7.638272
15	135615180	-110.192	-92.5983	-9.52507	7.69897
16	135472433	-113.898	-94.48	-12.5599	7.721246
17	136167958	-88.3328	-72.5388	-7.84053	7.60206
18	136167959	-120.065	-95.6446	-9.13858	7.356547
19	136167960	-88.8555	-77.9862	-8.97871	7.585027
20	136167961	-105.561	-89.1906	-6.59404	7.522879
21	136167962	-113.344	-100.078	-8.06497	7.60206
22	136167963	-100.612	-87.5822	-6.4142	7.769551
23	135501372	-111.382	-89.9003	-14.0372	7.69897
24	135567720	-99.8295	-84.9583	-7.40041	7.259637
25	136167964	-109.303	-77.8359	-5.31732	7.744727
26	136167965	-109.811	-92.2818	-4.6094	7.468521
27	136167966	-65.8516	-57.9782	-5.40971	7.769551
28	136167967	-115.947	-98.7885	-10.2071	8.0000
29	136167968	-119.068	-96.7145	-3.71361	7.823909
30	136167969	-109.308	-90.1535	-7.61707	7.958607
31	135643056	-112.878	-93.1477	-12.6721	7.744727
32	135495624	-115.944	-93.45	-8.83322	7.744727
33	136167970	-106.775	-82.3462	-9.25927	7.920819
34	136167971	-122.579	-99.9712	-9.69997	7.823909
35	136167972	-97.9948	-83.8592	-9.05978	7.886057
36	136167973	-125.369	-94.2108	-6.98926	8.221849
37	136167974	-122.327	-96.5416	-9.55364	7.920819
38	136167975	-110.912	-95.0911	-7.0041	7.853872
39	136167976	-125.217	-101.447	-10.1414	7.408935
40	135589440	-109.42	-87.5492	-8.4688	7.552842
41	135439717	-109.652	-95.1131	-12.8027	7.568636
42	136167977	-120.726	-93.7324	-15.3615	7.638272
43	135628628	-115.113	-96.273	-12.8103	7.721246

44	136167978	-93.5574	-79.7109	-13.9175	8.221849
45	135518293	-121.244	-98.9777	-6.5755	7.356547
46	136142892	-118.417	-100.942	-3.96015	7.455932
47	136167979	-113.333	-92.7264	-5.37359	7.468521
48	136167980	-114.883	-101.334	-16.5551	7.508638
49	136167981	-111.508	-91.2383	-16.8394	7.657577
50	136167982	-117.013	-95.1832	-9.35174	7.744727
51	136167983	-120.695	-103.17	-10.2973	7.744727
52	135815951	-99.0165	-84.5465	-7.75534	8.00000
53	136167984	-113.767	-88.6878	-10.0765	7.69897
54	136167985	-119.306	-95.5218	-4.51722	7.638272
55	136167986	-99.0991	-84.7398	-5.90487	7.568636
56	135521406	-104.808	-82.4659	-6.96394	7.958607
57	135615174	-101.164	-81.7865	-10.2797	7.657577
58	135536260	-106.615	-90.9606	-6.88603	8.045757

The docking view of three representative compounds (39, 48, and 51) in the binding site of CMP are shown in Figure 2. Hydrogen bonding, hydrophobic and steric interactions are seen to be the character collaborations between the compounds and CMP. H-bond formation was found to occur between the amide (-CN bonds), nitro (-NO2 bonds) and carbonyl oxygen (-CO) of the compound 51- protein complex (Fig. 2A) with Gly37, Gly15, Gly17, and Arg131 respectively, and H-bonds were found between the Carbon-Fluorine bond of the compound 39 and the carbonyl oxygen of Thr20 and the carbonyl oxygen of compound 39 and CN Asp129, Asp35, Lys18, Gly15, Gly17, Ala16, and Gly37 respectively, which strengthens the binding interaction (Fig. 2B). H-bonds were also found between the hydroxyl oxygen of the compound 48 and the carbonyl oxygen of Thr20 and CN of Gly19, Lys23, and Thr20 respectively, which also strengthens the binding interaction (Fig. 2C). The hydrogen-bonding strongly determines the 3D space position of the benzene ring in the binding pocket and enables the hydrophobic interaction of compound 51 with the side chain of Ser14 and 36, Asp132, Tyr40, Asp35 and 129, Lys18, Gly19, Arg157, Ala16, Pro13 and Gly130 (Fig. 2A). It can, therefore, be concluded that the NO-2 ions of the molecules facilitate them to bind with CMP.

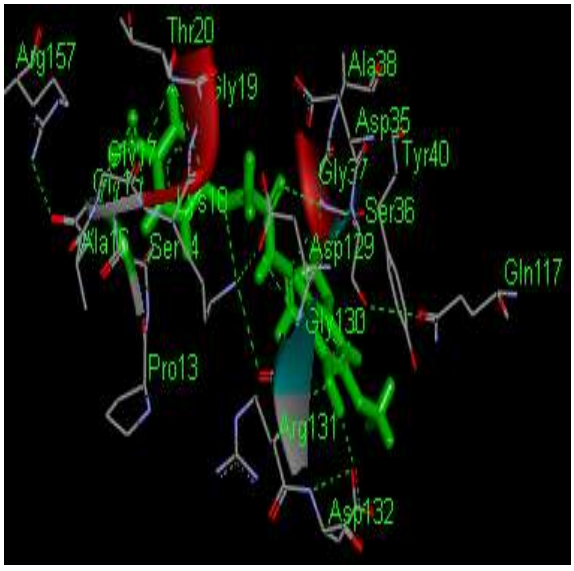

A

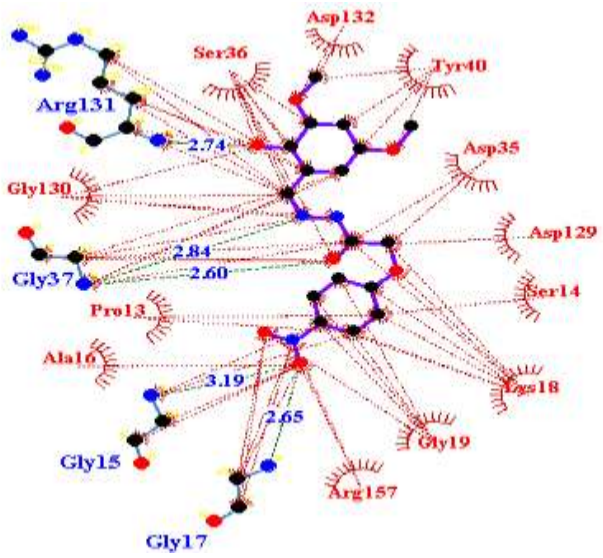

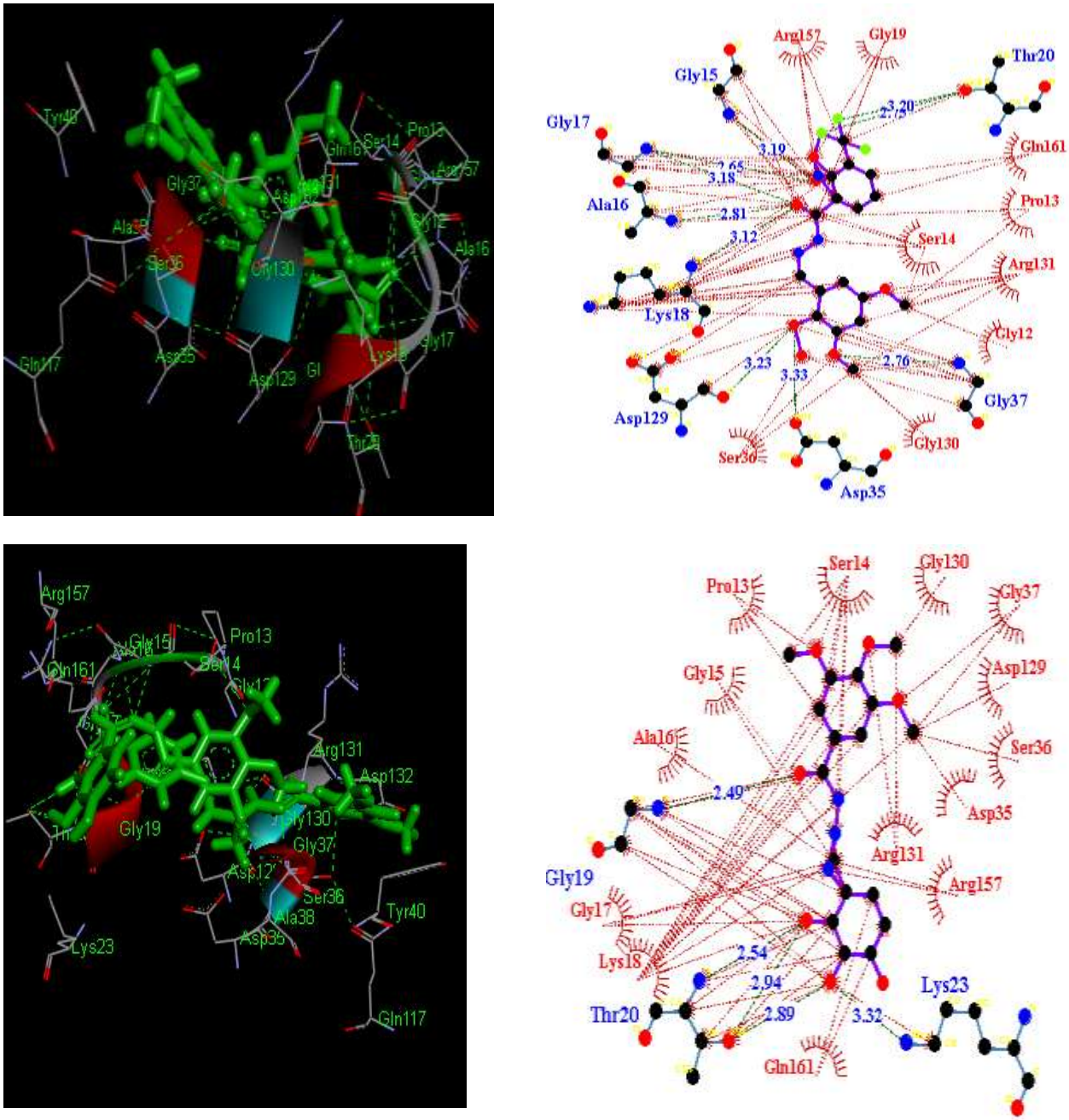

Figure 2. Docking views of (A) compound 51, (B) compound 39, and (C) compound 48 and hydrophobic interaction between compound 51 and CMP in the binding site. The green dotted line shows H-bonds. Carbon is colored in black, oxygen red, and nitrogen blue. Ligand bond, Non-ligand bond, Hydrogen bond and its length, Non-ligand residues involved in hydrophobic contacts, Corresponding atoms involved in hydrophobic contacts. (For interpretation of the references to color in this figure legend, the reader is referred to the web version of this article).

The three novel compounds (39, 48, and 51) were predicted with the modification of compounds based on the results of molecular docking. The result of MD simulations demonstrated the dependability of the protein-ligand complex and gave extra data about the coupling method of compound 51. The temperature, total energy, and kinetic plot (Fig. 3), the root mean square deviation (RMSD) plot of the complex during the MD simulations are shown in Figure 3D. This result of simulation demonstrated that the docking of active ligand was done accurately in the active site of CMP. It additionally gave the possibility that the compound 51 formed a stable complex with protein when protein was simulated up to or beyond 100ps concerning temperature (at or above 310 K), potential energy (at or below -48653.22 kJ/mol) kinetic energy (at or above 14495.1 kJ/mol) and total energy (at or above -34158.12 kJ/mol).

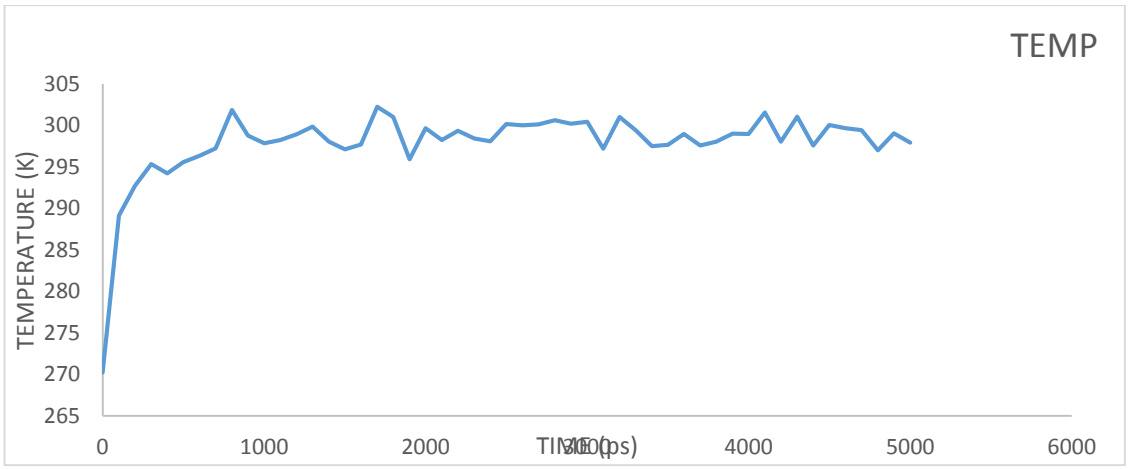
TEMP
TEMPERATURE (K)
305
300
295
290
285
280
275
270
265
0
1000
2000
4000
5000
6000

A

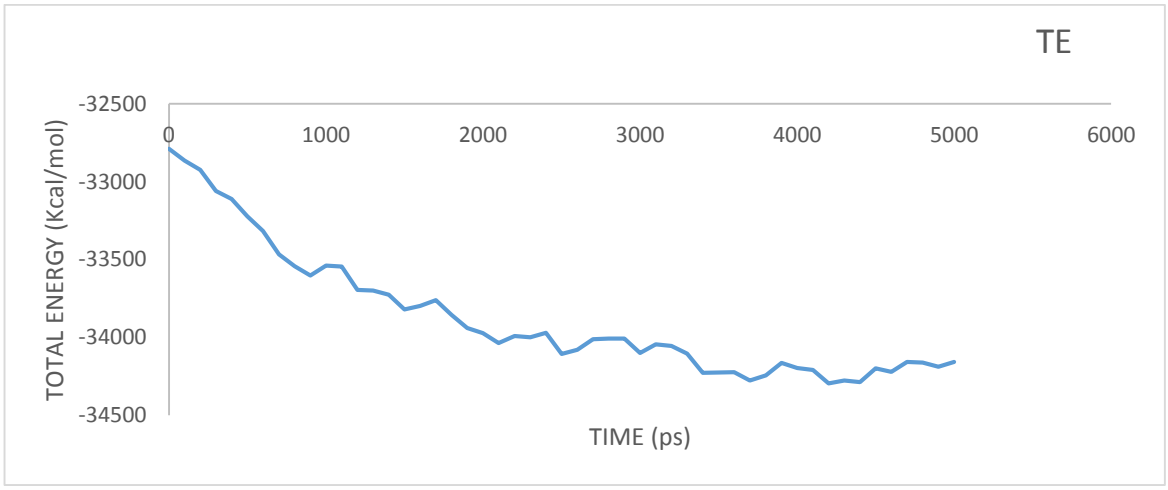
TE
TOTAL ENERGY (Kcal/mol)
-32500
-33000
-33500
-34000
-34500
0
1000
2000
3000
4000
5000
6000
TIME (ps)

B

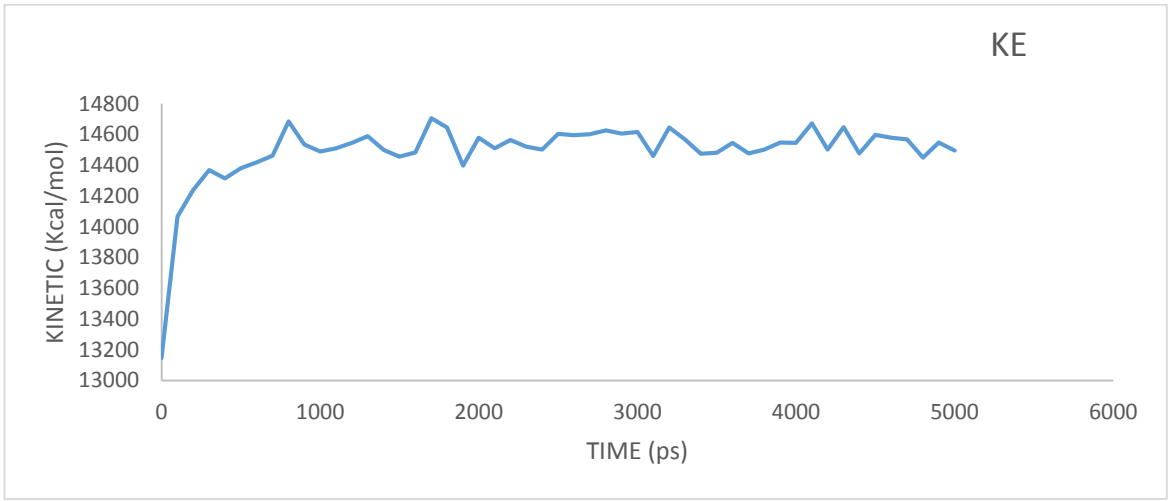
KE
KINETIC (Kcal/mol)
14800
14600
14400
14200
14000
13800
13600
13400
13200
13000
0
1000
2000
3000
4000
5000
6000
TIME (ps)

C

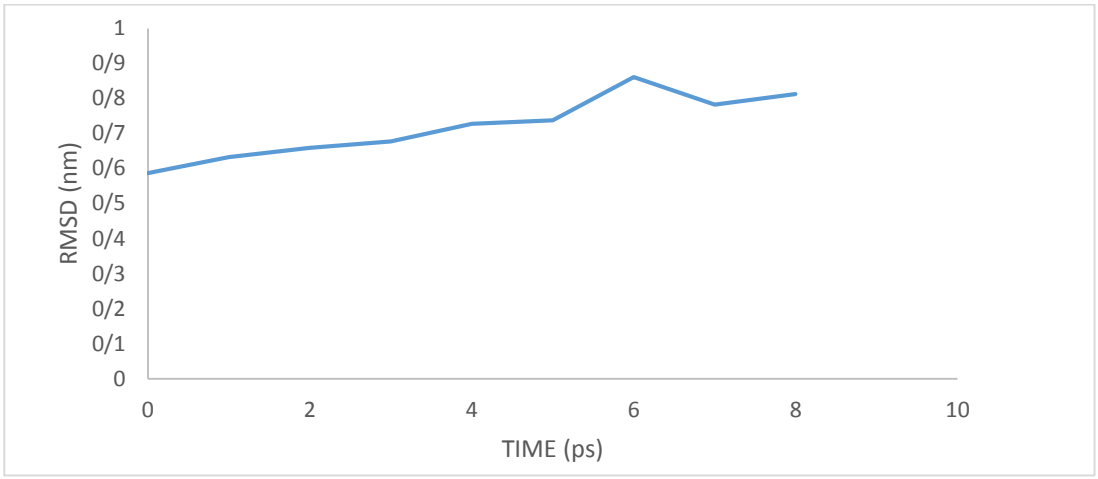

Figure 3. Molecular dynamics simulations study of A-chain of protein CMP (PDB ID: 4e22) concerning (A) time versus temperature; (B) time versus potential energy; (C) time versus kinetic energy; (D) RMSD values of protein backbone for CMP complex during 100ps MD simulation

We looked at the compliance of the complex after simulation with the initial. As shown in Figure 2A, compound 51 adopts a similar pose and was placed in the same region of two structures, which means that the compound can be stably located in the docking site. And then, we compared the residues which interact with compound 51 after the simulation. As shown in Figures 4 and 5 respectively, compound 51 went deeper into the CMP binding pocket and this would significantly increase the binding affinity. Compound 51 formed a series of hydrogen bonds with Arg131, Thr20, and Gly17 at the distance of 2.97 Å, 3.22 Å, and 2.62 Å respectively.

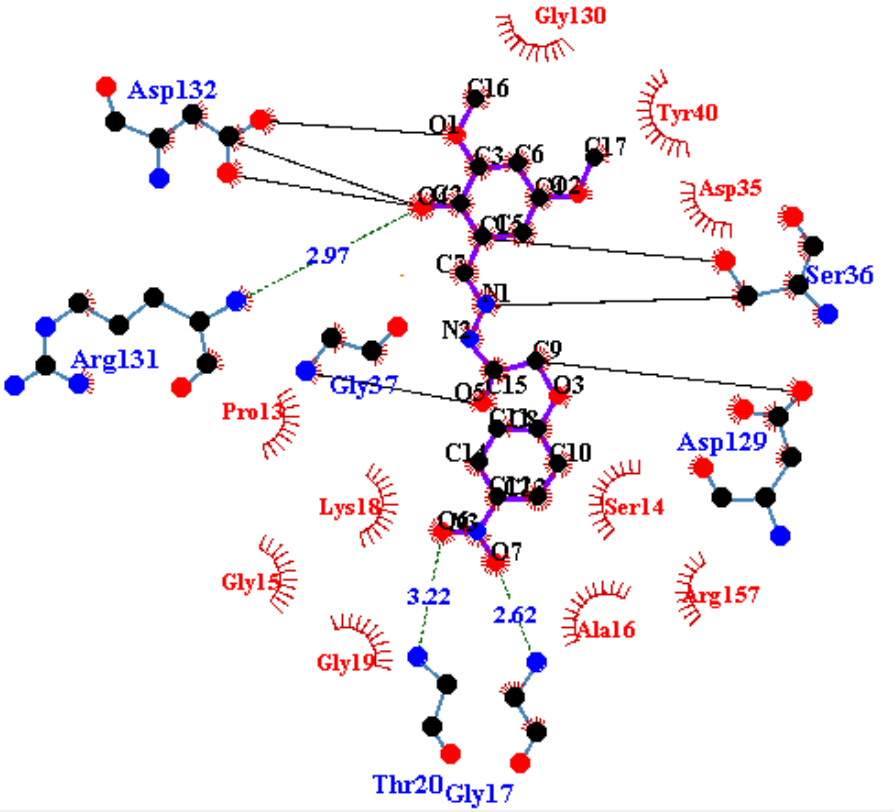

Figure 4. The binding mode of compound 51 with CMP after MD simulation. Compound 51 and surrounding residues were shown in the Ligplus model. Hydrogen bonds were shown in blue dash lines.

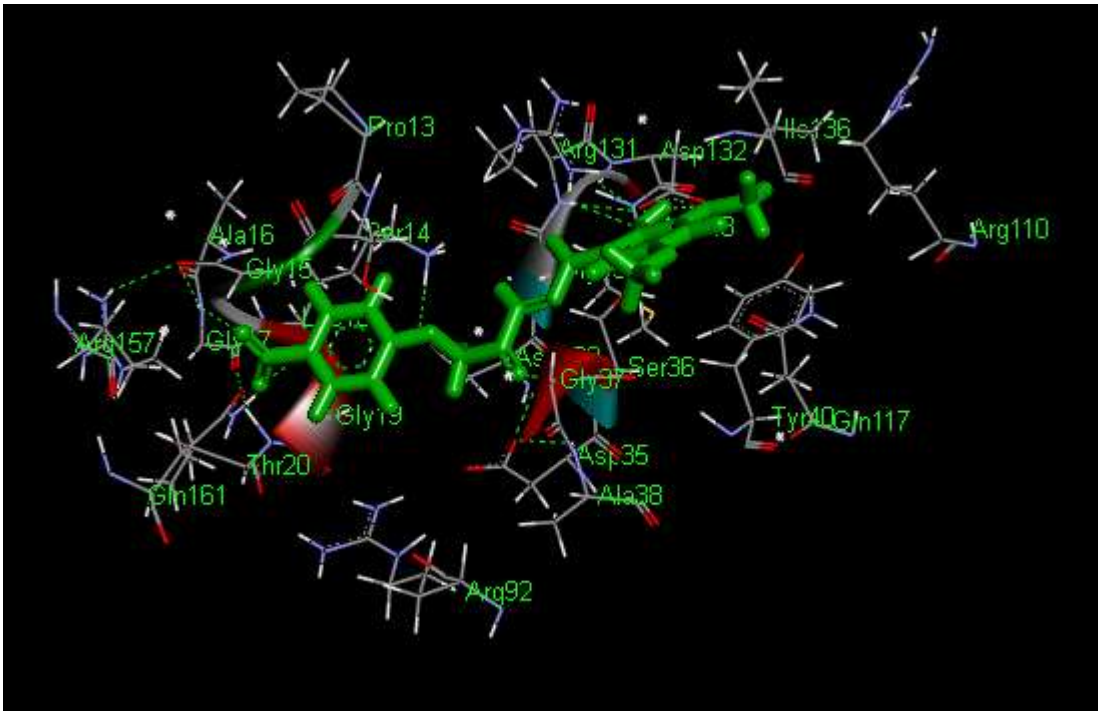

Figure 5. Result of molecular dynamics simulations during the 5 ns NVT ensemble plot of the protein-ligand complex.

2.1 Multi-Parameter Optimization (MPO) and Drug-Like of salicylidene acylhydrazides derivatives

An indispensable goal for this statement was to assess the physicochemical domain on 58 derivatives of salicylidene acylhydrazides (Table 1). The properties involved are Partition coefficient octanol/water (log P), molecular weight (MWt), hydrogen bond donors (HBD), hydrogen bond acceptors (HBA), number of rotatable bonds (nrotb), polar surface area (PSA), Ligand efficiency (LE) and Lipophilic efficiency (LipE). The outcomes were determined utilizing Spartan14 v1.1.4, PaDEL v2.20, PowerMV v0.61 [37] and MedChem Designer v3.1.0.30 [38] are shown in Table 2-4. These parameters permit recognizing the oral assimilation or layer porousness that happens when the considered atom meets the Lipinski's "rule of five" (molecular weight (MWt) $\leq$ 500 Da, log P $\leq$ 5, H-donor (HBD) $\leq$ 5 and acceptors H (HBA) $\leq$ 10) [23, 39] and Veber's rule [24]. The molecules which don't follow more than one of these conditions may have bioavailability challenges and a high likelihood of outperforming drug assorted variety. The rules are based on a strong physicochemical justification. Hydrogen bonds increase solvency in water and should be broken for the compound to penetrate into and through the lipid bilayer layer [40]. Therefore, an increasing number of hydrogen bonds reduce partitioning from the aqueous phase into the lipid bilayer membrane for penetration by passive diffusion. Salicylidene acylhydrazides derivatives are under the rule, except compounds 1, 4, 11, 14, 20, 25-27, 29, 30, 36-38, 44, and 47 as shown in Table 2, so we can say that the rest compounds are probably more polar and hardly absorbed. The number of rotating bonds (NumRot) is a descriptor of the oral bioavailability of the drugs; it measures the molecular flexibility [24]. The rotator joins are characterized as a solitary non-ring bond, bound to the non-hydrogen charges. Amide C–N bonds are not considered due to their high energy barrier in the rotation [41]. Notably, high oral bioavailability is a significant factor for the advancement of bioactive molecules as therapeutic agents. Reduced molecular flexibility and low polar surface area are seen as significant indicators of good oral bioavailability [40]. Though, rotatable bonds and polar surface areas tend to increase with molecular weight to a limited extent clarify the achievement of these two parameters in foreseeing the oral bioavailability and the transport across membranes. The low number of rotatable bonds in the studied series indicates that these Ligands upon binding to a protein change their conformation only slightly. Molecular flexibility relates to the ease by which the molecule transverses the membrane [24]. The number of rotatable bonds of a successful drug is < 8 [42]. All the compounds of our antibiotics inhibitors series have NumRot < 8, except the compounds 15, 37, 45, 46, and 51 their NumRot is 8, 9 respectively (Table 2). Then again, the polar surface area (PSA) is formed by polar atoms of a molecule. Polar surface area (PSA) is a descriptor that shows a good correlation with passive molecular transport through membranes, thus permits estimation of transport properties of drugs [43]. In the examined arrangement of salicylidene acylhydrazides derivatives, the high estimations of PSA bring about the exacerbating of the assimilation of a drug. Compound 19 with PSA values

145.24 belongs to the compounds with reduced absorption (Table 2). Molecular weight (MWt) is identified with the size of the particle. As molecular size increases, a larger cavity must be formed in water to solubilize the compound. Increasing MWt diminishes the compound concentration at the outside of the intestinal epithelium, in this way lessening ingestion. Expanding size additionally thwarts detached dissemination through the firmly pressed aliphatic side chains of the bilayer layer [44, 45]. Some series of salicylidene acylhydrazides derivatives with molecular weights (Table 3) less than 500 Da (except compound 12, 13, and 14) so they are likely soluble and easily pass through cell membranes. The determination of the stability of different molecular conformations in water solutions depends on their hydration energy, though the prediction of drug transport properties depends on total polar surface area (TPSA) [46]. It is a parameter that has a decent connection with human intestinal absorption, the single-layer permeability of Caco-2, and the penetration of the blood-brain barrier [47]. Molecules with TPSA values of 140Å2 or more should show poor intestinal absorption [48]. TPSA values Table 2 calculated by PaDeL v2.20 especially compound 51 were found to be 126.04, get an opportunity to cross the BBB, and have better bioavailability. T_PSA values Table 3 were calculated by MedChem designer v3.0 especially compounds 39, 48, and 51, PubChem_CID: 136167974, 136167980, and 136167963 respectively, were found in the range of 80.15-135.2, these get an opportunity to cross the BBB and have better bioavailability. We can notice that all exhibited a great percentage of absorption (%ABS) Table 4 [49] ranging from 24.32 to 65.52%, indicating that these compounds should have good cellular plasmatic membrane permeability.

Table 2. Physico-chemical parameters of salicylidene acylhydrazides derivatives

Compound	nHeavyAtom	TPSA	BBB	NumHBA	NumHBD	NumRot	PSA	XLogP
1	23	108.511	1	4	2	6	61.69	4.224
2	20	148.835	1	4	2	5	61.69	2.994
3	19	---------	0	4	2	4	74.58	1.674
5	23	139.744	1	4	2	5	61.69	4.345
5	22	154.041	0	7	2	5	78.76	1.67
6	21	126.377	0	5	2	5	124.94	3.254
7	21	--------	0	5	2	5	83.81	1.914
8	18	202.040	0	6	2	5	94.71	1.213
9	22	162.985	0	5	2	5	70.92	2.907
10	20	139.330	1	4	2	4	61.69	2.667
11	24	108.859	1	4	2	5	61.69	5.632
12	24	141.082	0	6	2	6	80.15	3.863
13	23	141.795	0	5	2	6	70.92	3.588
14	22	118.933	0	4	2	4	61.69	4.537
15	26	137.593	0	8	2	8	98.61	2.297
16	23	127.689	0	8	2	6	87.99	2.005
17	23	315.127	0	7	5	6	122.38	1.323
18	24	280.567	0	6	4	4	130.39	2.318
19	17	395.560	0	8	5	4	145.24	-0.59
20	23	178.718	1	4	2	5	61.69	2.544
21	24	139.079	0	8	2	7	87.99	1.759
22	21	166.769	0	5	2	5	70.92	1.693
23	19	128.662	0	4	2	4	115.71	3.014
24	16	211.212	0	5	2	4	85.48	0.973
25	25	136.422	0	5	2	6	70.92	4.313
26	23	115.292	1	4	2	5	61.69	4.073
27	27	111.654	1	4	2	6	61.69	7.038
28	24	174.124	0	6	2	6	80.15	2.51
29	23	194.081	1	4	2	6	61.69	2.375

30	22	155.364	1	4	2	4	61.69	3.184
31	26	116.937	0	7	2	7	89.38	3.211
32	23	105.742	0	7	2	5	78.76	2.919
33	23	223.401	0	6	3	7	91.15	1.725
34	24	178.126	0	5	2	5	99.16	2.72
35	17	210.518	0	7	3	5	114.01	-0.188
36	30	118.342	1	4	2	7	61.69	5.972
37	31	115.4507	0	8	2	9	87.99	5.187
38	28	97.3774	0	5	2	7	70.92	5.121
39	26	157.014	0	6	2	7	80.15	2.908
40	23	-------	0	8	2	6	100.88	1.378
41	20	185.264	0	9	2	6	111.78	0.677
42	27	132.904	0	11	2	7	105.06	3.622
43	25	80.076	0	10	2	6	95.83	3.382
44	29	133.027	0	10	2	7	95.83	6.347
45	27	120.044	0	7	2	9	83.39	3.197
46	26	197.290	0	6	2	9	74.16	2.922
47	25	98.974	1	5	2	7	64.93	3.871
48	26	245.447	0	9	4	7	129.84	2.753
49	23	223.743	0	9	4	5	119.22	2.461
50	24	211.521	0	6	3	7	91.15	2.478
51	27	126.040	0	10	2	9	106.45	2.123
52	18	223.747	0	7	3	5	114.01	0.565
53	24	156.711	0	7	2	7	89.38	2.057
54	25	116.354	0	5	2	5	99.16	3.473
55	19	--------	0	4	2	4	74.58	1.498
56	20	140.849	1	4	2	4	61.69	2.878
57	21	164.818	0	5	2	5	70.92	2.33
58	22	132.679	0	5	2	6	70.92	3.234

Table 3. Pharmacological activities and properties involved in MPO method for salicylidene acylhydrazides derivatives.

Compound	MlogP	S+logP	S+logD	RuleOf5	RuleOf5_Code	MWt	M_NO	T_PSA	HBDH
1	4.196	4.663	4.659	1	LP	310.398	4	61.69	2
2	3.874	4.039	4.03	0	<None>	333.191	4	61.69	2
3	2.463	3.358	3.334	0	<None>	320.152	5	74.58	2
4	4.464	5.223	5.219	1	LP	310.398	4	61.69	2
5	3.422	3.541	3.456	0	<None>	303.251	7	107.51	2
6	1.562	2.912	2.739	0	<None>	371.219	7	96.7	2
7	1.944	2.971	2.934	0	<None>	350.178	6	83.81	2
8	1.713	2.626	1.065	0	<None>	312.129	6	94.71	2
9	3.594	4.51	4.485	0	<None>	383.636	5	70.92	2
10	4.142	4.702	4.682	0	<None>	353.609	4	61.69	2
11	4.54	5.69	5.686	1	LP	346.859	4	61.69	2
12	3.4	5.095	4.549	1	Mw	552.108	6	80.15	2
13	4.059	5.233	5.078	1	Mw	540.072	5	70.92	2
14	4.96	6.043	5.78	2	Mw,LP	560.945	4	61.69	2
15	1.433	2.828	2.772	0	<None>	360.369	8	98.61	2
16	2.801	2.948	2.873	0	<None>	315.287	8	116.74	2
17	1.7	2.293	2.066	0	<None>	316.316	7	122.38	5
18	2.161	4.127	3.756	0	<None>	362.793	6	102.15	4

19	-0.401	0.926	0.444	1	Hb	239.189	8	145.24	6
20	4.262	4.632	4.567	1	LP	326.252	4	61.69	2
21	2.926	3.232	3.066	0	<None>	333.278	8	116.74	2
22	3.108	3.83	3.794	0	<None>	288.28	5	70.92	2
23	2.053	3.188	3.097	0	<None>	341.192	6	87.47	2
24	1.941	2.711	0.977	0	<None>	282.103	5	85.48	2
25	4.284	5.363	5.349	1	LP	405.299	5	70.92	2
26	4.847	5.558	5.551	1	LP	375.272	4	61.69	2
27	4.928	6.271	6.269	1	LP	368.523	4	61.69	2
28	2.822	4.144	3.806	0	<None>	352.752	6	80.15	2
29	4.5	4.788	4.743	1	LP	338.743	4	61.69	2
30	4.382	5.113	4.935	1	LP	361.589	4	61.69	2
31	2.414	4.386	3.701	0	<None>	399.233	7	89.38	2
32	3.798	4.058	3.934	0	<None>	354.151	7	107.51	2
33	2.703	3.14	3.133	0	<None>	314.343	6	91.15	3
34	3.171	4.751	4.735	0	<None>	360.821	5	70.92	2
35	0.382	1.648	1.636	0	<None>	237.216	7	114.01	4
36	5.932	7.079	7.076	1	LP	420.478	4	61.69	2
37	4.647	5.972	5.97	1	LP	427.504	8	116.74	2
38	4.829	6.436	6.434	1	LP	382.506	5	70.92	2
39	3.057	3.872	3.852	0	<None>	368.314	6	80.15	2
40	1.414	2.761	1.296	0	<None>	316.275	9	129.63	2
41	1.146	2.105	-0.004	0	<None>	278.226	9	140.53	2
42	3.077	3.723	1.394	1	NO	439.186	11	162.56	2
43	3.554	3.811	1.558	0	<None>	409.159	10	153.33	2
44	4.239	4.982	2.378	1	LP	402.409	10	153.33	2
45	2.641	3.733	3.728	0	<None>	371.439	7	83.39	2
46	3.287	3.88	3.875	0	<None>	359.403	6	74.16	2
47	4.172	4.952	4.941	1	LP	380.276	5	64.93	2
48	0.456	2.553	1.951	0	<None>	362.341	9	129.84	4
49	1.806	2.521	1.92	0	<None>	317.26	9	147.97	4
50	3.057	3.632	3.608	0	<None>	393.244	6	91.15	3
51	1.823	2.656	2.644	0	<None>	375.34	10	135.2	2
52	1.084	2.124	2.06	0	<None>	316.117	7	114.01	4
53	1.944	3.005	2.996	0	<None>	330.343	7	89.38	2
54	3.517	5.053	4.994	0	<None>	439.722	5	70.92	2
55	2.334	3.256	3.232	0	<None>	275.696	5	74.58	2
56	4.142	4.624	4.597	0	<None>	353.609	4	61.69	2
57	3.354	4.18	4.164	0	<None>	349.191	5	70.92	2
58	3.594	3.864	3.841	0	<None>	363.218	5	70.92	2

Hydration energy is a significant component deciding the stability of different molecular conformations in water solutions [40]. Hydration energy (HF) in absolute value (Table 4), the most elevated is that of compound 39, in the organic situations the polar atoms are encircled by water particles. They are set up hydrogen bonds between them. Models, for example, ligand productivity (LE), which relates power and size, and ligand-lipophilicity proficiency (LLE), which connects intensity and lipophilicity, have been used by restorative physicists to altogether assess compound strength to properties [50]. Ligand-proficiency subordinate lipophilicity (LELP), a capacity that associates each of the three components of power, size, and lipophilicity, and the desirable range for LELP, $-10 < LELP < 10$ for acceptable leads [50]. The broadly acknowledged lower breaking point of ligand effectiveness (LE) has been 0.3 [51], and the lipophilicity (LogP) run for lead-like mixes is $LogP \leq 5$ [52], LogP was determined to gauge the hydrophobicity of compounds. Compound with high lipophilicity and high logP will have a poor surface collaboration with the gut and likely poor assimilation. It is realized that mixes with a $\log P < 5$ can be retained well. The outcomes acquired by figuring LogP of salicylidene acylhydrazides subordinates utilizing Spartan14 programming show that our computations of LogP values are seen as in the range. If the lipophilicity is too high, there is an increased likelihood of binding to other targets than those desired

and, therefore, there is more potential for toxicity [53]. Table 4 shows that all the compounds are arranged in the recommended run – 10 < LELP < 10 aside from compound 37 with LELP of 11.909. On the opposite side, all the mixes have LELP under 16.5, which implies that these mixes are in the Lipinski zone (ROF-score = 4). Table 4 shows that 100% of the medications have LipE esteem > 3.3 [25]. Excellent mixes have higher LipE values as indicated by Ryckmans and his associates [54]. Therefore, all the compounds are deemed to be the optimal compounds.

Table 4. Drug-likeness parameters percentage of absorption and and properties involved in MPO method of salicylidene acylhydrazides derivatives.

Compound	LogP <5	%ABS	HF (Kcal/mol)	LE	LipE	LELP
21	1.01	61.018	-361.59	0.443	6.592	2.278
28	3.44	48.927	-541.34	0.467	4.56	7.371
29	4.21	42.042	-476.16	0.476	3.614	8.840
34	4.39	47.546	-143.88	0.456	3.434	9.619
37	4.26	69.170	-388.17	0.358	3.661	11.909
39	3.64	54.830	-1009.59	0.399	3.769	9.124
45	3.68	67.585	-400.97	0.381	3.677	9.647
46	3.68	40.935	-435.77	0.401	3.776	9.166
48	1.82	24.321	-821.10	0.404	5.689	4.501
51	0.59	65.516	-486.93	0.402	7.154	1.469

%ABS = 109 ± 0.345 × TPSA [49]; LE = 1.4 × PIC50/NH [51]; LipE = PIC50 – LogP [53]; LELP = LogP/LE [50]

The Golden Triangle can be utilized as a device to affect the plan of new focuses by accomplishing a higher likelihood of drug-like space [26]. The probability of success in maximizing potency, stability, and permeability is realized by moving the design properties into an area with a baseline of MlogP and S+logD = 0 to 7 at MWt = 450, these limits give a triangular shape, called the golden triangle. For our series of molecules, it is obvious that compounds 21, 28, 29, 34, 37, 39, 45, and 46 have great penetrability and low clearance since they are focused inside the golden triangle area (Fig. 6 and 7). According to the results obtained by these rules, these compounds (21, 28, 29, 34, 37, 39, 45, and 46) have the highest probability of success in maximizing potency, stability, and permeability

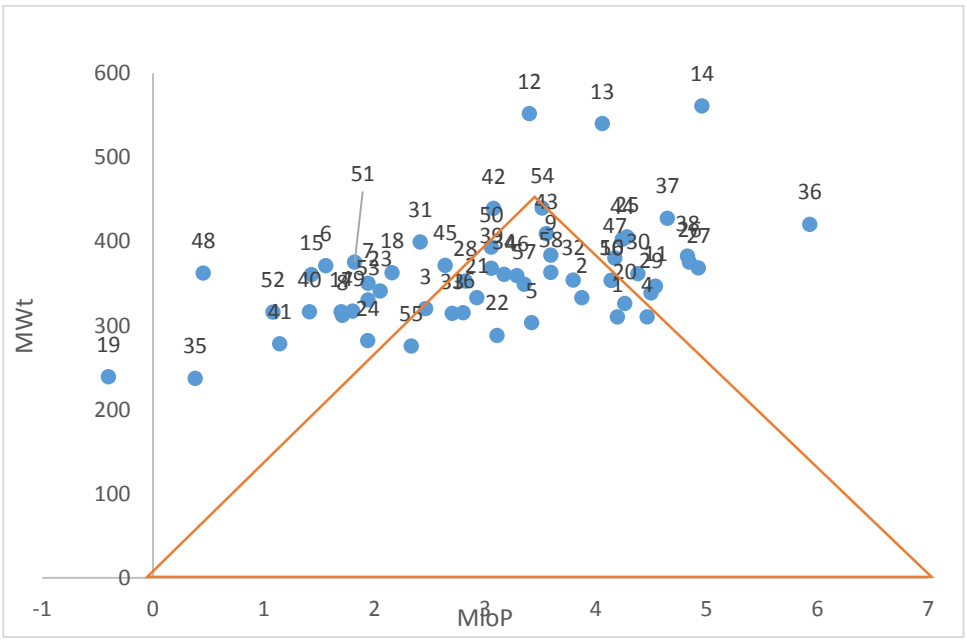

Figure 6. In vitro permeability and clearance trends across MWt and MlogP.

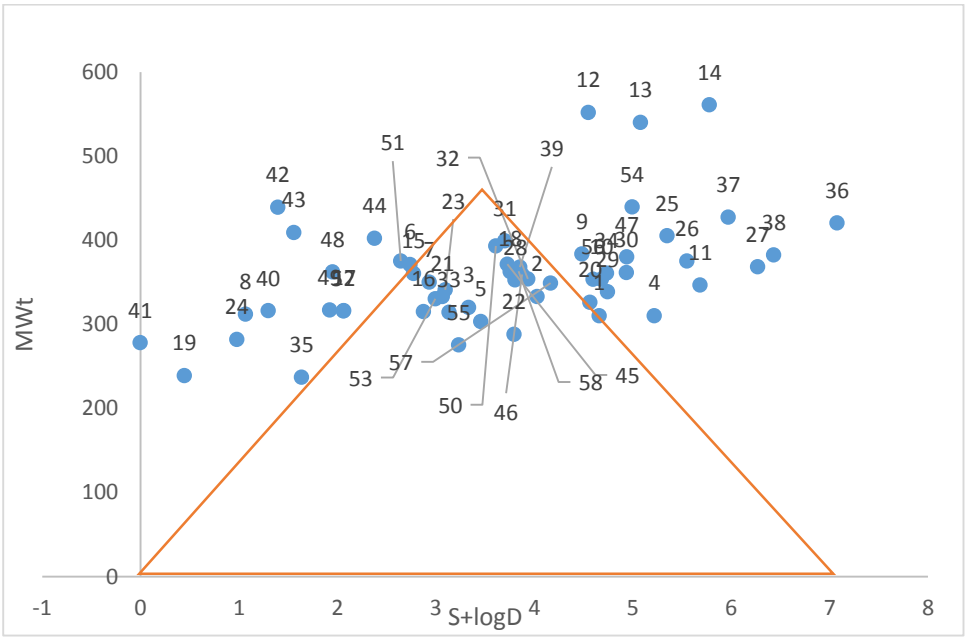

Figure 7. In vitro permeability and clearance trends across MWt and S+logD.

3. Principle and methodology

3.1. Database and biological activity

The set of 58 salicylidene acylhydrazides derivatives [27], as inhibitors of type III secretion (T3S) in the Gram-negative pathogen Yersinia pseudotuberculosis was compiled from the PubChem (https://pubchem.ncbi.nlm.nih.gov/bioassay/473049) [28]. The IC50 (uM) values of the type III secretion (T3S) in the Gram-negative pathogen Yersinia pseudotubrculosis and Chlamydia trachomatis inhibitor activity data of salicylidene acylhydrazides derivatives were converted into the negative logarithmic scale (log(1/IC50)). That is, pIC50 values were used for calculation in this paper (pIC50 = - log IC50= log(1/ IC50). The PubChem_CID numbers, MVD docking are shown in Table 1.

3.2. Molecular docking and Molecular dynamic simulation

The binding mode for the compounds to cytidine monophosphate (CMP) kinase (PDB entry code: 4e22) [29] was studied by Molegro Virtual Docker (MVD). A limit of 10 conformers was considered for each compound, during the docking process. All the MVD docking runs were performed in Pentium (R) Dual-Core CPU @ 2.30 GHz of DELL system origin, with 3.00GB RAM 64-bit Operating System, an x64-based processor. MVD was compiled and run under Microsoft Windows 10 Pro operating system. The crystal structure of cytidine monophosphate (CMP) kinase (PDB entry code: 4e22) [29] was extracted from the Brook haven Protein Database (PDB http://www.rcsb.org/pdb).

To additionally demonstrate the dependability of our docking results and affirm the steadiness of the complex of protein-ligand, molecular dynamics (MD) simulations study was performed with the CHARMM27 force field using the NAMD package [30]. Molecular dynamics simulations are carried out with periodic boundary conditions [31]. Minimization was performed to optimize the initial structure of the protein-ligand complex. After that, the temperature of the system was gradually heated up from 0 K to 310K in 100 ps. along these lines, the system was equilibrated at 310K for 100ps with the NVT ensemble.

All the initial geometries of the compounds were minimized and optimized by semi-empirical method PM6 wavefunction/spartan's 14 v1.1.4 [32], at that point the geometries of generated structures were re-optimized using MMFF94 force field as implemented in the PaDEL-Descriptor version 2.20 software [26]. The quantum chemical descriptors, including the energy of the highest occupied molecular orbital (EHOMO), the energy of the lowest unoccupied molecular orbital (ELUMO), the formation energy (HF), solvation energy (SE), standard enthalpy (H^o) and entropy (S^o), and Gibb's energy (G^o) in the molecule were computed by Spartan 14 [33].

4. Conclusion

In this study, molecular docking, molecular dynamics simulation, virtual screening, and ADMET approaches were employed to predict and find the probable lead compounds from virtual screening. Docking studies were performed using Melogro virtual docker (MVD) programs to obtain the bioactive conformations for the whole dataset. In MVD docking the ligand with the highest potency (compound 51) forms four hydrogen bonds with residues of flexible joint region amino acids Arg131, Gly15, Gly17, and Gly37. Despite this, Molecular dynamic simulation was done and analyses

such as RMSD, temperature, total energy, and kinetic energy, displayed that proposed compound 51 is stable in the CMP active sites. The use of MPO desirability score, Lipinski, Veber, lipophilicity indices (Table 2-4) and golden triangle rules approaches (Fig. 7,8) showed that the compound 51 has a better BBB permeation, good intestinal permeability, and oral bioavailability, they have a desired in vitro ADME and safety attributes. These results help us to design a successful drug, with better anti- Yersinia pseudotuberculosis and Chlamydia trachomatis activity. This information could be of high value for the design and development of novel multi-targeted drugs against Yersinia pseudotuberculosis and Chlamydia trachomatis possessing improved binding properties and low toxicity to human cells.

Conflict of Interest

The author(s) confirm that this article content has no conflict of interest.

Acknowledgements

The authors gratefully acknowledge the Department of Chemistry, Ahmadu Bello University, Zaria (Samaru, Zaria-Nigeria); for computational studies, and as part of the Ph.D. thesis.

References

[1] W.H.O. Multidrug and extensively drug-resistant tuberculosis: Global report on surveillance and response. World Health Organization; Geneva, Switzerland (2010).

[2] F. J. Prado-Prado, E. Uriarte, F. Borges, H. Gonza´ lez-Dı´az, Multi-target spectral moments for QSAR and Complex Networks study of antibacterial drugs. *European Journal of Medicinal Chemistry*, 44 (2009) 4516–4521.

[3] N. J. Walker, E. A. Clark, D. C. Ford, H. L. Bullifent, E. V. McAlister, M. L. Duffield, K. R. Acharya, P. C. Oyston, Structure and function of cytidine monophosphate kinase from Yersinia pseudotuberculosis, essential for virulence but not for survival. 2(12) (2012) 120142. doi: 10.1098/rsob.120142 DOI: 10.1098/rsob.120142.

[4] M. Achtman, K. Zurth, C. Morelli, G. Torrea, A. Guiyoule, E. Carniel, Yersinia pestis, the cause of plague, is a recently emerged clone of Yersinia pseudotuberculosis. *Proc. Natl Acad. Sci.*, 96 (1999) 14043–14048. doi:10.1073/pnas.96.24.14043.

[5] V. Kumar, A. K. Abbas, N. Fausto, R. N. Mitchell, Robbins Basic Pathology, 8th ed.; Saunders Elsevier: Philadelphia, PA (2007).

[6] www.medicalnewstoday.com

[7] Centers for Disease Control and Prevention MMWR Morbidity Mortality Weekly Report, CDC, 2015. Sexually Transmitted Diseases Treatment Guidelines, 2015 Recommendations and Reports Vol. 64 (3), June 5.

[8] L. B. Rice, Unmet medical needs in antibacterial therapy. *Biochem Pharmacol*., 71(7) (2006) 991–995.

[9] S. A. Siadati, N. Nami, & M. R. Zardoost, A DFT study of solvent effects on the cycloaddition of norbornadiene and 3,4-dihydroisoquinoline-N-oxide. *Progress in Reaction Kinetics and Mechanism*, 36(3) (2011) 252-258.

[10] M. R. Zardoost, & S. A. Siadati, A DFT study on the effect of functional groups on the formation kinetics of 1,2,3-triazolo-1,4-benzoxazine via intramolecular 1,3-dipolar cycloaddition. *Progress in Reaction Kinetics and Mechanism*, 38(2) (2013) 191-196.

[11] M. R. Zardoost, S. A. Siadati, & B. G. Oghani, A DFT study on the 1,3-dipolar cycloaddition of benzonitrile oxide and N-ethylmaleimide. *Progress in Reaction Kinetics and Mechanism*, 38(3) (2013) 316-322.

[12] E. I. Edache, A. Uzairu, P. A. P. Mamza and G. A. Shallengwa, Prediction of HemO Inhibitors Based on Iminoguanidine using QSAR, 3DQSAR Study, Molecular Docking, Molecular Dynamic Simulation and ADMET. *J Drug Design Discov Res*, 1(2) (2020) 36-52.

[13] E. I. Edache, A. Uzairu, P. A. Mamza and G. A. Shallengwa, A comparative QSAR analysis, 3D-QSAR, molecular docking and molecular design of iminoguanidine-based inhibitors of HemO: A rational approach to antibacterial drug design. *J. Drugs Pharm. Sci.*, 4(3) (2020) 21-36.

[14] S. A. Siadati, M. Afzali, & M. Sayyadi, Could silver nano-particles control the 2019-nCoV virus? An urgent glance to the past. *Chem. Rev. Lett.*, 3(1) (2020) 9-11.

[15] S. A. Siadati, M. A. Rezvanfar, E. Babanezhad, A. Beheshti, & M. Payab, Harmony of operations of some vitamins in controlling the 2019-nCoV virus based on scientific reports, *Chem. Rev. Lett.*, 3 (2020) 202-206.

[16] L. Turski, in Virtual ADMET Assessment in Target Selection and Maturation (Eds.: B. Testa, L. Turski) IOS Press, (2006) Washington, DC.

[17] M. Abbasi, F. Ramezani, M. Elyasi, H. Sadeghi-Aliabadi, M. Amanlou, A study on quantitative structure–activity relationship and molecular docking of metalloproteinase inhibitors based on L-tyrosine scaffold. *DARU Journal of Pharmaceutical Sciences*. 23(1): (2015) 1–10.

[18] C. Hansch, A. Kurup, R. Garg, H. Gao, Chem-bioinformatics and QSAR: a review of QSAR lacking positive hydrophobic terms. *Chem. Rev*. 101(3): (2001) 619–72.

[19] R. T. Kroemer, Structure-based drug design: docking and scoring. *Current Protein and Peptide Science*, 8(4): (2007) 312–28.

[20] L. G. Ferreira, R. N. dos Santos, G. Oliva, A. D. Andricopulo, Molecular Docking and Structure-Based Drug Design Strategies. *Molecules*, 20 (2015) 13384-13421; https://doi: 10.3390/molecules200713384.

[21] S. Kalyaanamoorthy, Y. P. Chen, Structure-based drug design to augment hit discovery. *Drug Discov. Today*, 16 (2011) 831–839.

[22] M. Segall, Multi-parameter optimization: identifying high quality compounds with a balance of properties. *Curr. Pharm. Des.*, 18 (2012) 1292.

[23] C. A. Lipinski, F. Lombardo, B. W. Dominy, P. J. Feeney, Experimental and computational approaches to estimate solubility and permeability in drug discovery and development settings. *Adv. Drug Deliv. Rev*., 23: (1997) 3–25.

[24] D. F. Veber, S. R. Johnson, H. Y. Cheng, B. R. Smith, K. W. Ward, K. D. Kopple, Molecular properties that

influence the oral bioavailability of drug candidates. *J. Med. Chem*., 45 (2002) 2615–2623.
[25] T. T. Wager, X. Hou, P. R. Verhoest, A. Villalobos, Moving beyond rules: the development of a central nervous system multiparameter optimization (CNS MPO) approach to enable alignment of druglike properties. *ACS Chem. Neurosci*., 1 (2010) 435–449.
[26] T. W. Johnson, K. R. Dress, M. Edwards, Using the Golden Triangle to optimize clearance and oral absorption. *Bioorg. Med. Chem. Lett*., 19 (2009) 5560–5564.
[27] S. Kim, J. Chen, T. Cheng, A. Gindulyte, J. He, S. He, Q. Li, B. A. Shoemaker, P. A. Thiessen, B. Yu, L. Zaslavsky, J. Zhang, E. E. Bolton, PubChem update: improved access to chemical data. *Nucleic Acids Res*., 47(D1) (2019) D1102-1109. doi:10.1093/nar/gky1033. [PubMed PMID: 30371825].
[28] National Center for Biotechnology Information. PubChem Database. Source=ChEMBL, AID=473049, https://pubchem.ncbi.nlm.nih.gov/bioassay/473049 (accessed on July. 07, 2019).
[29] E. A. Clark, K. R. Acharya, Structure of cytidine monophosphate kinase from Yersinia pseudotuberculosis (2012). DOI: 10.2210/pdb4e22/pdb Primary publication DOI: 10.1098/rsob.120142.
[30] J. C. Phillips, R. Braun, W. Wang, J. Gumbart, E. Tajkhorshid, E. Villa, C. Chipot, R. D. Skeel, L. Kale, K. Schulten, Scalable Molecular Dynamics with NAMD. *J. Comput. Chem*., 26(16) (2005) 1781-1802.
[31] M. P. Allen, D. J. Tildesley, Computer Simulations of Liquids. Clarendon Press: (1987) Oxford.
[32] Wavefunction, Inc. Spartan'14, (2014) version 1.1.4, Irvine, California, USA. www.wavefun.com.
[33] C. W. Yap, PaDel –Descriptor: An open source software to calculate molecular descriptors and fingerprints. *J. Comput. Chem*. 32(7) (2011) 1466-1474.
[34] S. Ray, P. B. Madrid, P. Catz, E. Susanna, L. Valley, M. J. Furniss, Development of a new generation of 4-aminoquinoline antimalarial compounds using predictive pharmacokinetic and toxicology models. *Journal of Medicinal Chemistry*, 53 (2010) 3685–3695.
[35] S. Kusumaningrum, E. Budianto, S. Kosela, W. Sumaryono, F. Juniarti, The molecular docking of 1,4-naphthoquinone derivatives as inhibitors of Polo-like kinase 1 using Molegro Virtual Docker. *J. App. Pharm. Sci*., 4 (11) (2014) 047-053.
[36] A. R. Puspaningtyas, Docking studies of Physalis peruviana ethanol extract using molegro virtual docker on insulin tyrosine kinase receptor as antidiabetic agent. *International Current Pharmaceutical Journal*, 3(5) (2014) 265-269.
[37] K. Liu, J. Feng, S. S. Young, PowerMV: A Software Enviroment for Molecular Viewing, Descriptor Generation, Data Analysis and Hit Evaluation. *J. Chem. Inf. Model*., 45: (2005) 515-522.
[38] MedChem Designer™ version 3.1.0130. www.simulations-plus.com
[39] P. Artursson, J. Karlsson, Correlation between oral drug absorption in humans and apparent drug permeability coefficients in human intestinal epithelial (Caco-2) cells, *Biochem Biophys Res Commun*., 175 (1991) 880–885.
[40] A. Rouane, N. Tchouar, A. Kerassa, S. Belaidi, M. Cinar, Structure-Based Virtual Screening and Drug-Like of Quercetin Derivatives with Anti-Malaria Activity. *Reviews in Theoretical Science*, 5 (2017) 1–11. doi:10.1166/rits.2017.1090.
[41] Z. Haddadi, H. Meghezzi, A. Amar, DFT and QSAR investigations of substituent effects in pyrazolooxazine derivatives: Activity prediction. *Journal of Theoretical and Computational Chemistry*, 18 (2019) 1950001. https://doi:10.1142/S0219633619500019.
[42] H. Pajouhesh, G. R. Lenz, Medicinal chemical properties of successful central nervous system drugs. *Neuro Rx*. 2 (2005) 541–553.
[43] T. Salah, S. Belaidi, N. Melkemi, N. Tchouar, Molecular Geometry, Electronic Properties, MPO Methods and Structure Activity/Property Relationship Studies of 1,3,4-Thiadiazole Derivatives by Theoretical Calculations. *Reviews in Theoretical Science*, 3 (2015) 1–10.
[44] F. Atkinson, S. Cole, C. Green, H. Van de Waterbeemd, Lipophilicity and other parameters affecting brain penetration. *Cent. Nerv. Syst. Agents. Med. Chem*., 2 (2002) 229–240.
[45] H. Van de Waterbeemd, G. Camenisch, G. Folkers, J. R. Chretien, O. A. Raevsky, Estimation of blood-brain barrier crossing of drugs using molecular size and shape, and H-bonding descriptors. *J. Drug Target*, 6 (1998) 151–165.
[46] N. Bodor, C. K. Shim, A new method for the estimation of partition coefficient, *J. Am. Chem. Soc.*, 111 (1989) 3783–3786.
[47] P. Ertl, B. Rohde, P. Selzer, Fast calculation of molecular polar surface area as a sum of fragment-based contributions and its application to the prediction of drug transport properties, *J. Med. Chem.*, 43 (2000) 3714–3717.
[48] V. N. Viswanadhan, A. K. Ghose, G. R. Revankar, R. K. Robins, Atomic physicochemical parameters for three dimensional structure directed quantitative structure-activity relationships.4. Additional parameters for hydrophobic and dispersive interactions and their application for an automated superposition of certain naturally occurring nucleoside antibiotics, *J. Chem. Inf. Comput.*, 29 (1989) 163–172.
[49] Y. H. Zhao, M. H. Abraham, J. Le, A. Hersey, C. N. Luscombe, G. Beck, I. Cooper, Rate-limited steps of human oral absorption and QSAR studies. *Pharmacol. Res*., 19 (2002) 1446–1457.
[50] G. M. Keserü, G. M. Makara, The influence of lead discovery strategies on the properties of drug candidates. *Nat. Rev. Drug Discov*., 8 (2009) 203–212.
[51] A. L. Hopkins, C. R. Groom, A. Alex, Ligand efficiency: a useful metric for lead selection. *Drug Discov. Today*, 9 (2004) 430–431.
[52] D. A. Smith, B. C. Jones, D. K. Walker, Design of drugs involving the concepts and theories of drug metabolism and pharmacokinetics. *Med. Res. Rev*., 16 (1996) 243–266.
[53] P. D. Leeson, B. Springthorpe, The influence of drug-like concepts on decision making in medicinal chemistry. *Nat. Rev. Drug Discov*., 6 (2007) 881–890.
[54] T. Ryckmans, M. P. Edwards, V. A. Horne, A. M. Correia, D. R. Owen, L. R. Thompson, I. Tran, M. F. Tutt, T. Young, Rapid assessment of a novel series of selective CB (2) agonists using parallel synthesis protocols: A lipophilic efficiency (LipE) analysis, *Bioorg. Med. Chem. Lett.*, 19 (2009) 4406–4409.